ROLE OF INDUCED MAGNETIC FIELD ON TRANSIENT NATURAL CONVECTION FLOW IN A VERTICAL CHANNEL: THE RIEMANN SUM APPROXIMATION APPROACH

B.K. JHA and I. SANI[*]
Department of Mathematics
Ahmadu Bello University, Zaria, NIGERIA
E-mail: basant777@yahoo.co.uk
sanimath@yahoo.com

This paper investigates the role of induced magnetic field on a transient natural convection flow of an electrically conducting, incompressible and viscous fluid in a vertical channel formed by two infinite vertical parallel plates. The transient flow formation inside the channel is due to sudden asymmetric heating of channel walls. The time dependent momentum, energy and magnetic induction equations are solved semi-analytically using the Laplace transform technique along with the Riemann-sum approximation method. The solutions obtained are validated by comparisons with the closed form solutions obtained for the steady states which have been derived separately and also by the implicit finite difference method. Graphical results for the temperature, velocity, induced magnetic field, current density, and skin-friction based on the semi-analytical solutions are presented and discussed.

Key words: induced magnetic field, natural convection flow, Riemann-sum approximation.

1. Introduction

Natural convection flows in vertical channels have been studied extensively because of their importance in many engineering applications, such as in accelerators, aerodynamic heating, electrostatic precipitation, polymer technology, petroleum industry, purification of crude oil and fluid droplet sprays to mention but a few. The works of Ostrach (1952) and Aung (1972) are among the early major contributions to the study of the convective flow and heat transfer in a vertical channel. Realizing the importance of transient convection in designing cooling systems using parallel plates, Joshi (1988) studied the transient effects in natural convection cooling of vertical parallel plates while Jha *et al.* (2003), Paul *et al.* (1996) and, Singh and Paul (2006) also carried out an extensive study on the free convective flow.

Literature survey also reveals that natural convection in an electrically conducting viscous fluid subject to an externally applied magnetic field has also received significant attention. Hartmann (1937) analyzed the effect of a transverse uniform magnetic field on the flow of a viscous incompressible electrically conducting fluid exiting through parallel stationary plates that are insulated. Romig (1964) studied the influence of an electric and magnetic field on heat transfer to electrical conducting fluids. Soundalgekar (1965) discussed the hydromagnetic flow near an accelerated plate in the presence of magnetic field. Mishra and Mohapatra (1975) also studied the unsteady free convective flow from a vertical plate in the presence of a uniform transverse and induced magnetic field. Ghosh and Bhattacharjee (2000) investigated a steady Hartmann flow of a viscous incompressible electrically conducting fluid in a rotating channel in the presence of an inclined magnetic field taking into account the induced magnetic field. Krishna (2009) studied the analytical solution to the problem of a free convective flow of an electrically conducting fluid between two heated parallel plates in the presence of an induced magnetic field. Attia (1998; 2004) also

---

[*] To whom correspondence should be addressed

studied the influence of the magnetic field on the velocity and temperature fields of an unsteady Hartmann flow of a conducting Newtonian fluid between two infinite non-conducting horizontal parallel fixed and porous plates. Other works under different physical situations on the free convective flow in the presence of a magnetic field includes that of Poots (1961), Osterle and Young (1961), Raptis, *et al.* (2003), Ram *et al.* (2010), Oreper and Szekely (1983) amongst others. Jha and Apere (2011) considered the unsteady magnetohydrodynamic free convective Couette flow of a viscous incompressible electrically-conducting fluid between two parallel vertical porous plates. Recently, Jha and Apere (2012) carried out a theoretical analysis of an unsteady magnetohydrodynamic free-convective flow of a viscous incompressible and electrically conducting fluid between two concentric vertical cylinders considering the thermal boundary condition of the second kind at the outer surface of the inner cylinder.

Moreover, the role of the induce magnetic field is of importance in many important problems in geophysics, astrophysics, cosmical and geophysical fluid dynamics as well as in many engineering processes. Nadeem and Akbar (2010) studied the influence of heat transfer and the induced magnetic field on a peristaltic flow of a Johnson-Segalman fluid in a vertical channel. An analytical solution to the problem of an MHD free convective flow of an electrically conducting fluid between two heated parallel plates in the presence of an induced magnetic field is analyzed by Singha (2009). An exact solution for a hydromagnetic free convective flow with an induced magnetic field is presented by Gosh *et al*. (2010). Singh *et al*. (2010) analyzed the hydromagnetic free convection in the presence of an induced magnetic field. Singh and Singh (2012) considered the steady fully developed laminar natural convective flow in open-ended vertical concentric annuli in the presence of a radial magnetic field taking into account the induced magnetic field produced by the motion of an electrically conducting fluid. Takhar *et al*. (1999) considered induced magnetic field effects in transient laminar hydromagnetic boundary layer convection along an impulsively started semi-infinite at plate with an aligned magnetic field, indicating that a reduction in the magnetic Prandtl number will enhance the surface shear stress, surface component of the induced magnetic field and also the surface heat transfer. Koshiba *et al*. (2002) presented a detailed study of the large-scale pulsed MHD generator system flow including induced magnetic field effects. Gupta *et al*. (2005) analyzed the hydromagnetic steady shear flow along an electrically insulating porous at plate. They concluded that the velocity at a given point increases with an increase in either the magnetic field or suction velocity and the induced magnetic field at a given location is reduced with increasing the magnetic field. A nonsimilar, laminar, steady, electrically-conducting forced convection liquid metal boundary layer flow with induced magnetic field effects was presented by Beg (2009). Despite the contributions made so far in this area, little or no mention of the role of the induced magnetic field on the transient natural convection flow in a vertical channel is made.

The objective of the present work is to present a semi-analytical solution for a transient natural convection flow due to asymmetric heating of a vertical channel in the presence of induced magnetic field effects. The solutions of the governing equations are obtained using a combination of the Laplace transform technique and the Riemann-sum approximation method of Laplace inversion reported in Jha and Apere (2010).

2. Mathematical analysis

We consider a transient natural convection flow of an incompressible viscous fluid along the walls of a vertical channel. At time $t' \leq 0$ both the fluid and the channel walls are assumed to be at the same temperature T_0. At time $t' > 0$ the temperature of the wall at $y' = 0$ is raised to T_1 while that at the wall $y' = d$ is maintained at T_0. The x' - axis is taken along the channel walls in the direction of the flow and y' -axis taken normal to it. A uniform magnetic field of strength H_0 is applied perpendicular to flow direction. Using the Boussinesq's approximation, the mathematical model representing the present physical situation by taking into consideration the induced magnetic field is

$$\frac{\partial T'}{\partial t'} = \alpha \frac{\partial^2 T'}{\partial y'^2} \, , \tag{2.1}$$

$$\frac{\partial u'}{\partial t'} = \nu \frac{\partial^2 u'}{\partial y'^2} + \frac{\mu_e H_0}{\rho} \frac{\partial h'}{\partial y} + g\beta(T' - T_0), \tag{2.2}$$

$$\frac{\partial h'}{\partial t'} = \frac{1}{\sigma\mu_e} \frac{\partial^2 h'}{\partial y'^2} + H_0 \frac{\partial u'}{\partial y'} \, , \tag{2.2}$$

together with

$$t' \leq 0: \ u' = 0, \quad T' = T_0, \quad h' = 0, \quad \text{for} \quad 0 \leq y \leq d,$$

$$t' > 0: \begin{cases} u' = 0, & T' = T_1, & h' = 0 \quad \text{at} \quad y' = 0, \\ \\ u' = 0, & T' = T_0, & h' = 0 \quad \text{at} \quad y' = d \end{cases} \tag{2.4}$$

where u' is the velocity, h' is the induced magnetic field, H_0 is the applied magnetic field, T' is the temperature of the fluid, ν is the kinematic viscosity, g is the acceleration due to gravity, β is the coefficient of thermal expansion, μ_e is the magnetic permeability, ρ the density, α is thermal diffusivity of fluid. By introducing the following non-dimensional quantities

$$y = \frac{y'}{d}, \quad t = \frac{t'\nu}{d^2}, \quad u = \frac{u'\nu}{g\beta(T_1 - T_0)d^2}, \quad \text{Pr} = \frac{\nu}{\alpha}, \quad h = \frac{h'\left(\frac{\mu_e}{\rho}\right)^{\frac{1}{2}}\nu}{g\beta d^2(T_1 - T_0)},$$

$$\text{Pm} = \sigma\mu_e\nu, \quad \theta = \frac{(T' - T_0)}{(T_1 - T_0)}, \quad M = \frac{dH_0}{\nu}\left(\frac{\mu_e}{\rho}\right)^{\frac{1}{2}} \tag{2.5}$$

where u is the dimensionless velocity, h is the dimensionless induced magnetic field, t the dimensionless time, y is the dimensionless coordinate normal to the channel plates, θ is the dimensionless temperature, others are the magnetic parameter M, magnetic Prandtl number Pm and the Prandtl number Pr, the governing dimensionless equations are

$$\frac{\partial\theta}{\partial t} = \frac{1}{\text{Pr}} \frac{\partial^2\theta}{\partial y^2} \, , \tag{2.6}$$

$$\frac{\partial u}{\partial t} = \frac{\partial^2 u}{\partial y^2} + M\frac{\partial h}{\partial y} + \theta \, , \tag{2.7}$$

$$\frac{\partial h}{\partial t} = \frac{1}{\text{Pm}} \frac{\partial^2 h}{\partial y^2} + M\frac{\partial u}{\partial y} \, . \tag{2.8}$$

The corresponding initial and boundary conditions for the velocity, temperature and the induced magnetic field in a dimensionless form are;

$$t \leq 0: \quad u=0, \quad \theta=0, \quad h=0 \quad \text{for} \quad 0 \leq y \leq 1,$$

$$t > 0: \begin{cases} u=0, \quad \theta=1, \quad h=0, \quad \text{at} \quad y=0 \\ \\ u=0, \quad \theta=0, \quad h=0, \quad \text{at} \quad y=1 \end{cases} \tag{2.9}$$

The solution of Eq.(2.6) using initial and boundary conditions (2.9) for *Pm=1* can be obtained using the Laplace transform technique. By defining the following transform variables

$$\overline{\theta}(y,s) = \int_0^\infty \theta(y,t) e^{-st} dt, \tag{2.10}$$

$$\overline{u}(y,s) = \int_0^\infty u(y,t) e^{-st} dt, \tag{2.11}$$

$$\overline{h}(h,s) = \int_0^\infty h(h,t) e^{-st} dt, \tag{2.12}$$

where *s>0* is the Laplace parameter, we obtain the following ordinary differential equations

$$\frac{d^2\overline{\theta}}{dy^2} - sPr\overline{\theta} = 0, \tag{2.13}$$

$$\frac{d^2\overline{u}}{dy^2} + M\frac{d\overline{h}}{dy} - s\overline{u} = 0, \tag{2.14}$$

$$\frac{d^2\overline{h}}{dy^2} + M\frac{d\overline{u}}{dy} - s\overline{h} = 0. \tag{2.15}$$

The boundary conditions now become

$$\overline{u}=0, \quad \overline{\theta}=0, \quad \overline{h}=0, \quad \text{for} \quad 0 \leq y \leq 1 \quad \text{and} \quad t \leq 0,$$

$$t > 0: \begin{cases} \overline{u}=0, \quad \overline{\theta}=\dfrac{1}{s}, \quad \overline{h}=0 \quad \text{at} \quad y=0, \\ \\ \overline{u}=0, \quad \overline{\theta}=0, \quad \overline{h}=0 \quad \text{at} \quad y=1. \end{cases} \tag{2.16}$$

Therefore, the solutions of Eqs (2.13)-(2.15) are, respectively

$$\overline{\theta}(y,s) = \frac{\sinh\left(\sqrt{s\text{Pr}}\,(1-y)\right)}{s\sinh\left(\sqrt{s\text{Pr}}\right)}, \tag{2.17}$$

$$\overline{u}(y,s) = \frac{1}{2}\left[\left(c_1\cosh(\lambda y) + c_2\sinh(\lambda y)\right)e^{-\frac{M}{2}y} + \left(\left(c_3\cosh(\lambda y) + c_4\sinh(\lambda y)\right)e^{\frac{M}{2}y}\right)\right] +$$
$$+ \frac{\sinh\sqrt{s\text{Pr}}\,(1-y)(s\text{Pr}-s)}{s\sinh\left(\sqrt{s\text{Pr}}\right)\left[(s\text{Pr}-s)^2 - M^2 s\text{Pr}\right]}, \tag{2.18}$$

$$\overline{h}(y,s) = \frac{1}{2}\left[\left(c_1\cosh(\lambda y) + c_2\sinh(\lambda y)\right)e^{-\frac{M}{2}y} + \left(\left(c_3\cosh(\lambda y) + c_4\sinh(\lambda y)\right)e^{\frac{M}{2}y}\right)\right] +$$
$$+ \frac{M\sqrt{s\text{Pr}}\,\cosh\left(\sqrt{s\text{Pr}}\,(1-y)\right)}{s\sinh\left(\sqrt{s\text{Pr}}\right)\left[(s\text{Pr}-s)^2 - M^2 s\text{Pr}\right]}. \tag{2.19}$$

Equations (2.17)-(2.19) are to be inverted in order to obtain the temperature, the velocity and the induced magnetic field in the time domain. To achieve this, the method used in Jha and Apere (2010) which is based on the Riemann-sum approximation is employed, since the inverse of the Laplace transform is very difficult here. In this method, functions in the Laplace domain (*s*) can be inverted to the time domain as follows

$$\theta(y,t) = \frac{e^{\varepsilon t}}{t}\left[\frac{1}{2}\overline{\theta}(y,\varepsilon) + \text{Re}\sum_{k=1}^{N}\overline{\theta}\left(y,\varepsilon + \frac{ik\pi}{t}\right)(-1)^k\right], \tag{2.20}$$

$$u(y,t) = \frac{e^{\varepsilon t}}{t}\left[\frac{1}{2}\overline{u}(y,\varepsilon) + \text{Re}\sum_{k=1}^{N}\overline{u}\left(y,\varepsilon + \frac{ik\pi}{t}\right)(-1)^k\right], \tag{2.21}$$

$$h(y,t) = \frac{e^{\varepsilon t}}{t}\left[\frac{1}{2}\overline{h}(y,\varepsilon) + \text{Re}\sum_{k=1}^{N}\overline{h}\left(y,\varepsilon + \frac{ik\pi}{t}\right)(-1)^k\right] \tag{2.22}$$

where Re refers to the 'real part, $i = \sqrt{-1}$ is an imaginary number, *N* is the number of terms used in the Riemann-sum approximation and ε is the real part of the Bromwich contour that is used in inverting Laplace transforms. The Riemann-sum approximation for the Laplace inversion involves a single summation for the numerical process. Its accuracy depends on the value of ε and the truncation error dictated by *N*. According to Tzou (1997), the value of ε must be selected so that the Bromwich contour encloses all the branch points. For faster convergence the quantity $\varepsilon t = 4.7$ gives the most satisfactory results.

2.1. Skin friction and current density

The skin-friction and the current density are obtained by differentiating Eqs (2.21) and (2.22) with respect to *y*. Therefore, the following

$$\tau(y,t) = \frac{\partial u}{\partial y} = \frac{e^{\varepsilon t}}{t}\left[\frac{1}{2}\overline{u}_I(y,\varepsilon) + \text{Re}\sum_{k=1}^{N}\overline{u}_I\left(y,\varepsilon + \frac{ik\pi}{t}\right)(-1)^k\right]$$

where

$$\overline{u}_I = \frac{\lambda}{2}\left[(c_I\sinh(\lambda y) + c_2\cosh(\lambda y))e^{-\frac{M}{2}y} + (c_3\cosh(\lambda y) + c_4\sinh(\lambda y))e^{\frac{M}{2}y}\right] +$$

$$+\frac{M}{4}\left[(c_I\sinh(\lambda y) + c_2\cosh(\lambda y))e^{-\frac{M}{2}y} - (c_3\cosh(\lambda y) + c_4\sinh(\lambda y))e^{\frac{M}{2}y}\right] + \quad, \qquad (2.23)$$

$$-\frac{\sqrt{s\text{Pr}}\cosh\left(\sqrt{s\text{Pr}}(I-y)\right)\left[M^2\sqrt{s\text{Pr}} + (s\text{Pr} - s)\right]}{s\sinh\sqrt{s\text{Pr}}\left[(s\text{Pr} - s) - M^2 s\text{Pr}\right]}.$$

Therefore, the skin friction at $y=0$, and at $y=1$, are as follows

$$\tau\big|_{y=0} = \frac{\lambda}{2}[c_2 + c_4] + \frac{M}{4}[c_I - c_3] - \frac{\sqrt{s\text{Pr}}\cosh\sqrt{s\text{Pr}}\left[M^2\sqrt{s\text{Pr}} + (s\text{Pr} - s)\right]}{s\sinh\sqrt{s\text{Pr}}\left[(s\text{Pr} - s) - M^2 s\text{Pr}\right]}, \qquad (2.23a)$$

$$\tau\big|_{y=I} = \frac{\lambda}{2}\left[(c_I\sinh(\lambda) + c_2\cosh(\lambda))e^{-\frac{M}{2}} + (c_3\cosh(\lambda) + c_4\sinh(\lambda))e^{\frac{M}{2}}\right] +$$

$$+\frac{M}{4}\left[(c_I\sinh(\lambda) + c_2\cosh(\lambda))e^{-\frac{M}{2}y} - (c_3\cosh(\lambda) + c_4\sinh(\lambda y))e^{\frac{M}{2}}\right], \qquad (2.23b)$$

and

$$J = -\frac{\partial h}{\partial y} = \frac{e^{\varepsilon t}}{t}\left[\frac{1}{2}\overline{h}_I(y,\varepsilon) + \text{Re}\sum_{k=1}^{N}\overline{h}_I\left(y,\varepsilon + \frac{ik\pi}{t}\right)(-1)^k\right], \qquad (2.24)$$

$$\overline{h}_I = \left\{\lambda(c_I\sinh(\lambda y) + c_2\cosh(\lambda y)) - \frac{M}{2}(c_I\cosh(\lambda y) + c_2\sinh(\lambda y))\right\}e^{-\frac{M}{2}y} +$$

where

$$+\left\{\lambda(c_3\sinh(\lambda y) + c_4\cosh(\lambda y)) - \frac{M}{2}(c_3\cosh(\lambda y) + c_4\sinh(\lambda y))\right\}e^{\frac{M}{2}y} + \qquad (2.24a)$$

$$-\frac{2M\text{Pr}\cosh\sqrt{s\,\text{Pr}}(I-y)}{\sinh\sqrt{s\text{Pr}}\left[(s\text{Pr} - s)^2 - M^2 s\text{Pr}\right]}.$$

2.2. Validation of the method

In order to validate the accuracy of the Riemann-sum approximation method, we set out in this section to find the solution of the steady state and the implicit finite difference method, which should coincide with the transient solution at large time.

2.2.1. Steady-state solution

The steady state solutions are obtained by setting $\dfrac{\partial}{\partial t}()$ to zero in Eqs (2.6)-(2.8) as

$$\theta_s = 1 - y,$$

$$u_s = \frac{1}{2M}(c_5 - c_7) + \frac{1}{M^2} - \frac{y}{M^2} + \frac{1}{2}\left(c_8 e^{My} + c_6 e^{-My}\right), \tag{2.25}$$

$$h_s = \frac{1}{2M}(c_5 + c_7) + \frac{1}{M^3} - \frac{y}{M} + \frac{y^2}{M} - \frac{1}{2}\left(c_8 e^{My} + c_6 e^{-My}\right). \tag{2.26}$$

The steady-state skin-friction and the steady state current density are obtained as follows;

$$\tau_s = \frac{1}{2}(c_5 + c_7) + \frac{y^2}{2} - \frac{y}{2}, \tag{2.27}$$

$$\tau_s\big|_{y=0} = \tau_s\big|_{y=1} = \frac{1}{2}(c_5 + c_7), \tag{2.28}$$

$$J_s = \frac{M}{2}\left(c_8 e^{My} + c_6 e^{-My}\right) + \frac{1}{M} - \frac{y}{M} \tag{2.29}$$

where $c_1, c_2, c_3, c_4, c_5, c_6, c_7, c_8, d_1, d_2, d_3, d_4, d_5, d_6$ and λ are defined in the Appendix.

2.2.2. Numerical solutions

Here, the implicit finite difference method is used to ascertain the correctness of the Riemann-sum approximation method. The procedure adopted involves approximation of differential equations by the finite difference equations and then solving the difference equations subject to the prescribed initial and boundary conditions. Thus, Eqs (2.6)-(2.8) become

$$\frac{u(i,j) - u(i,j-1)}{\Delta t} = \frac{1}{(\Delta y)^2}\big[u(i+1,j) - 2u(i,j) + u(i-1,j)\big] +$$
$$+ \frac{M}{2\Delta y}\big[h(i+1,j) - h(i-1,j)\big] + \theta(i,j), \tag{2.30}$$

$$\frac{h(i,j) - h(i,j-1)}{\Delta t} = \frac{1}{Pm}\frac{1}{(\Delta y)^2}\big[h(i+1,j) - 2h(i,j) + h(i-1,j)\big] +$$
$$+ \frac{M}{2\Delta y}\big[u(i+1,j) - u(i-1,j)\big], \tag{2.31}$$

$$\frac{\theta(i,j) - \theta(i,j-1)}{\Delta t} = \frac{1}{Pr}\frac{1}{(\Delta y)^2}\big[\theta(i+1,j) - 2\theta(i,j) + \theta(i-1,j)\big]. \tag{2.32}$$

Here the indices i and j in this case refer to y and t respectively. The time derivative is replaced by the backward difference expression and the spatial derivative by the central difference expression. Equations (2.30)-(2.32) are solved using a system of linear algebraic equations by Thomas algorithm. The numerical process continues until a solution is approached by satisfying the following convergence criterion

$$\frac{\sum \left| A_{i,j-1} - A_j \right|}{M^* \left| A \right|_{max}} \leq 10^{-6} ,$$

with respect to the fluid velocity field and the induced magnetic field. Here $A_{(i,j)}$ is the fluid velocity field, the induced magnetic field or the temperature field. M^* is the number of interior grid points and $\left| A \right|_{max}$ is the maximum absolute value of $A_{(i,j)}$. In the course of numerical computations care must be taken in specifying the value of Δt in obtaining the steady state solution small enough to avoid instabilities, therefore for the present situation we set it as;

$$\Delta t = \text{Stabr} \times \left(\Delta y \right)^2 .$$

The parameter *Stabr* is determined by numerical experimentation in order to achieve convergence and stability of the solution procedure. Numerical experiments show that the value 2 is suitable for the present numerical computation. The numerical values obtained using the implicit finite difference method are in excellent agreement with numerical values obtained semi-analytically for the transient state using the Riemann-sum for the velocity field, induced magnetic field, current density and the skin friction for $Pm = 1$.

3.   Results and discussion

In order to get a physical insight into the problem, a MATLAB programme is written to compute and generate the graphs for the temperature, velocity, induced magnetic field, current density, and the skin-friction for various values of the parameter embedded in the problem. The results are presented graphically in Figs 1 to 17. The values of Pr=*0.71* and Pr=*7.0* are considered in the computation which correspond to air and water as a working fluid, respectively.

Figures 1-2 show the temperature for varying values of time (*t*) and Prandtl number (Pr) respectively. It is observed from Figs 1a and 1b that the temperature increases as time increases and ultimately attains a steady state in both cases of air and water. During the numerical computation, it is observed that the time required to reach a steady state is directly proportional to the Prandtl number. Also, it is observed that the temperature is higher near the left plate at *y=0* than at the right plate at *y=1*. This is as a result of a rise in the temperature at the left plate. A decrease in the temperature as the Prandtl number Pr increases is observed in Fig.2. The temperature decreases as Pr increases which is an expected phenomena, since an increase in Pr decreases thermal diffusivity of the fluid and this causes low heat penetration and a reduction of the thermal boundary layer.
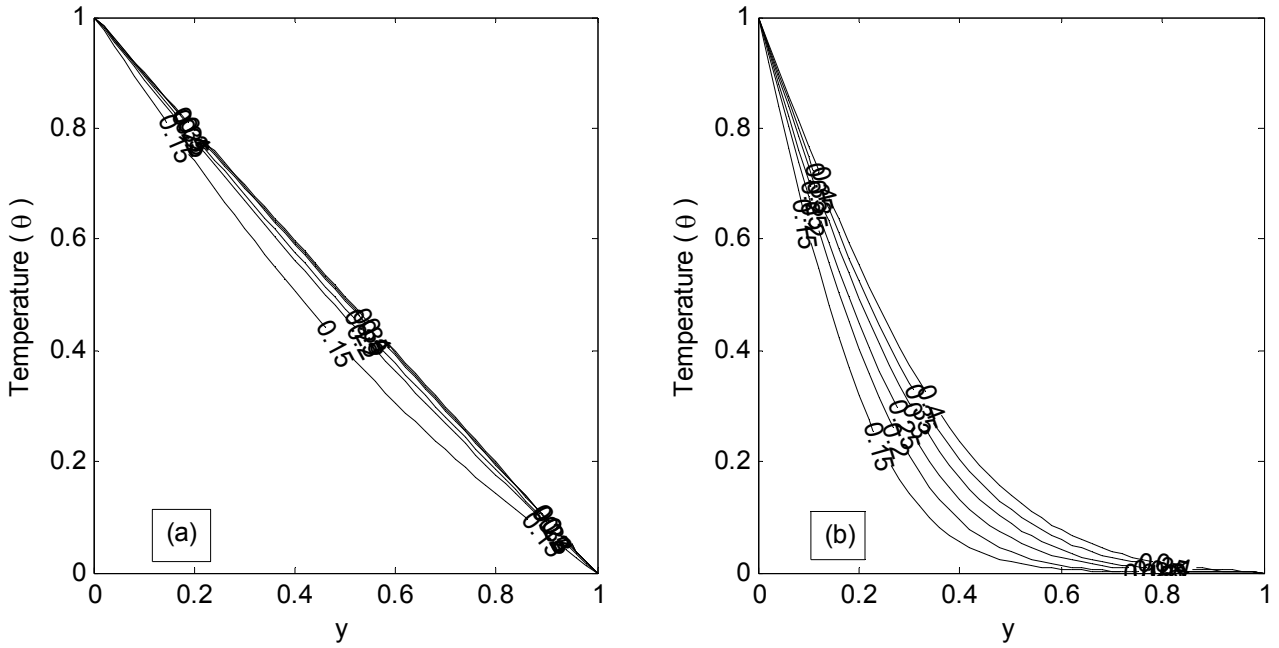
Fig.1. Temperature profiles at different values of time *t* for Pr=*0.71* (a) and *7.0* (b).
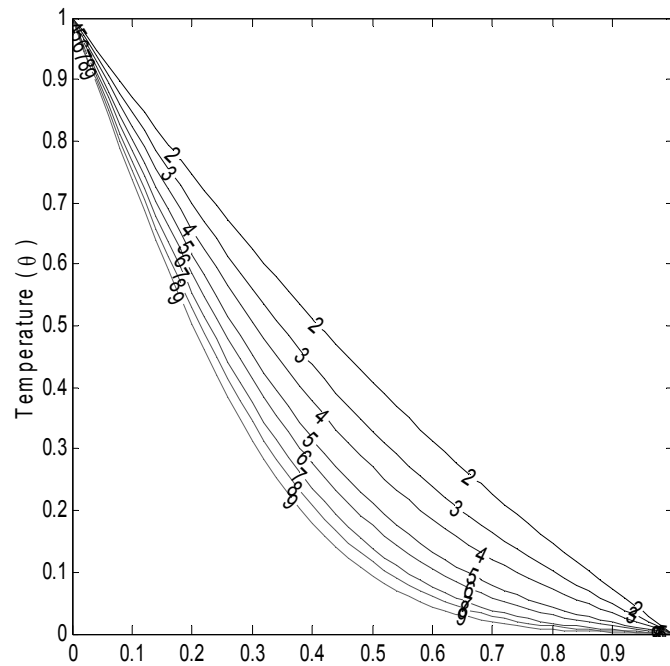
Fig.2. Temperature profiles at different values of Pr for *t=0.2*.

Figures 3-8 display the velocity and induced magnetic field in the channel for different values of dimensionless time (*t*), the magnetic parameter (*M*), and the Prandtl number (Pr). From Figs 3a and 3b it is observed that the velocity increases as time (*t*) increases and attains its steady state. These figures show that the time required to reach a steady state is higher in the case of water (Pr=*7.0*) than air (Pr=*0.71*). The velocity at varying values of the magnetic parameter (*M*) is illustrated in Fig.4. From Figs 4a and 4b it is clear that as *M* increases, velocity decreases in the central region and a reverse trend is observed near the

channel wall (*y=1*). This phenomenon is more visible in the case of water than air. This finding is very different from the general perception deduced from the Hartman flow which states that the external magnetic field produces the Lorentz force that inhibits the fluid motion. This result suggests that it is inappropriate to imagine the Lorentz force purely as a braking force, instead it would be more precise to think of the Lorentz force as a force that actually resists a change in motion due to external factors. It suggests that in the presence of the induced magnetic field, the magnetic parameter to accelerates the fluid motion. It is remarkable that for all magnetic parameters considered here, there exists a location inside the flow domain where the velocity field is independent of the magnetic parameter. The velocity variation with Pr is shown in Fig.5. It reveals that velocity decreases with an increase of Pr. This is attributed to the fact that as the Prandtl number (Pr) increases, thermal conductivity of the fluid decreases, causing a weak convection current.
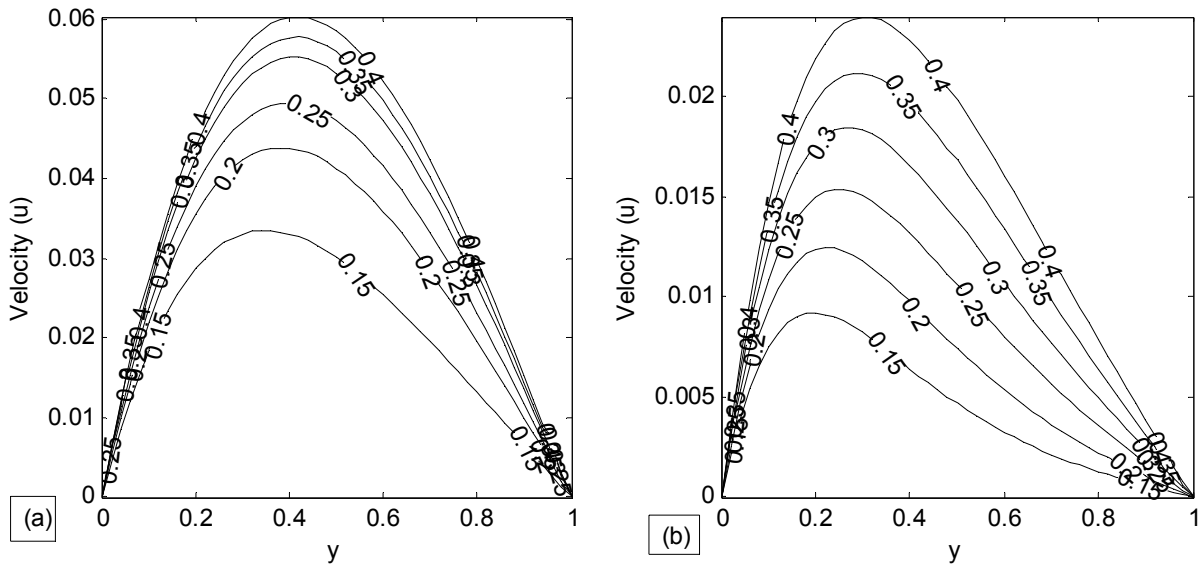
Fig.3. Velocity profiles at different values of time *t* for *M=0.5*, Pr=*0.71* (a) and *7.0* (b).
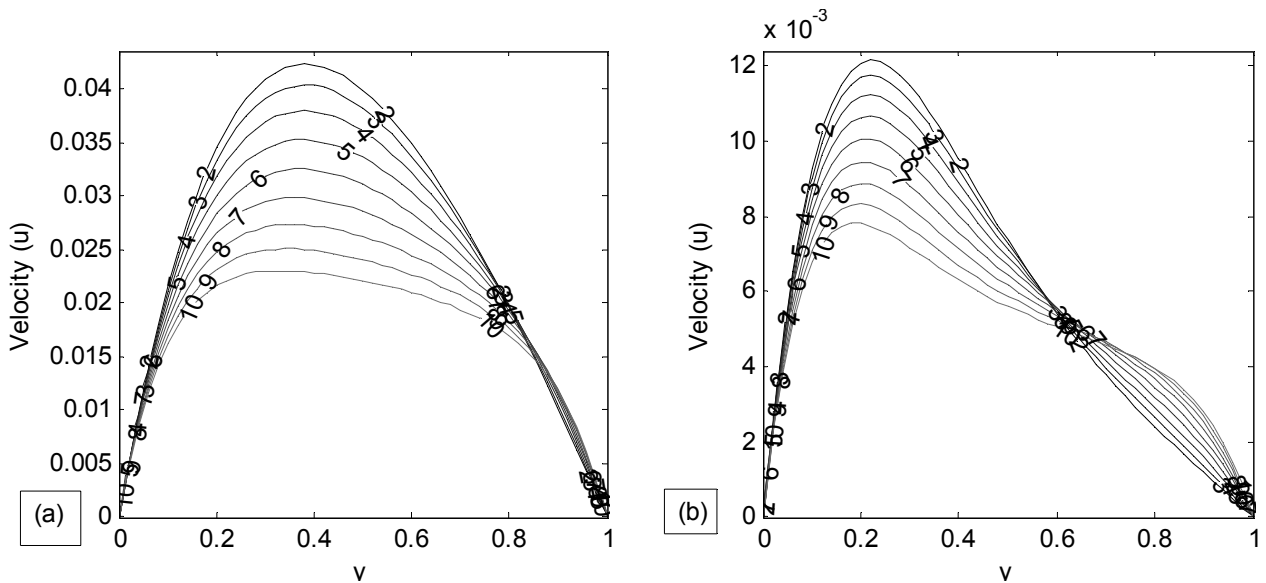
Fig.4. Velocity profiles at different values of *M* for *t=0.2*, Pr=*0.71* (a) and *7.0* (b).
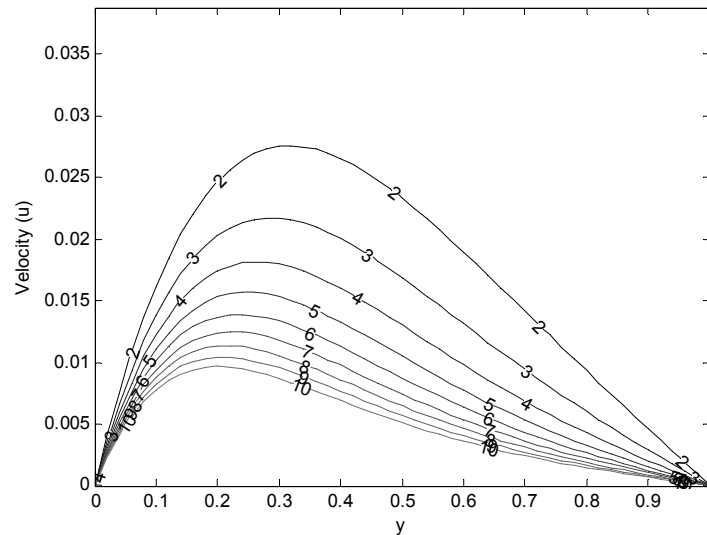
Fig.5. Velocity profiles at different values of Pr for *t=0.2, M=0.5*.

Figures 6-8 exhibit the behaviour of the induced magnetic field at different values of dimensionless time (Pr), the magnetic parameter (*M*) and the Prandtl number (Pr). The induced magnetic field is of a parabolic type in upward and downward direction in all cases assuming both positive and negative values. Figure 6a reveals that as time increases the induced magnetic field increases in the range *0 < y < 0.4* while it decreases in the range *0.4 < y < 1*. A similar behaviour is observed in Fig.6b with a shift in the location of inflection point (approximately *y=0.25*). This indicates an existence of a location where the induced magnetic field is independent of time. Also, this particular location is strongly dependent on the nature of the working fluid. Furthermore, it is seen from Fig.7a that the strength of the induced magnetic field is directly proportional to the strength of the magnetic parameter in the region *0 < y < 0.3* while it is inversely proportional in the region *0.3 < y < 1*. Also, in Fig.7b, a similar behaviour is noticed with a shift in the location of inflection point (approximately *y=0.15*). Hence, we conclude that there exists a point in the flow domain where the induced magnetic field is independent of the magnetic field applied. Also, the point of inflection where the induced magnetic field changes its character is strongly dependent on the nature of the working fluid. Variations of the induced magnetic field with Prandtl number are shown in Fig.8. From this figure, it is evident that the induced magnetic field increases as well as decreases with an increase of Pr.
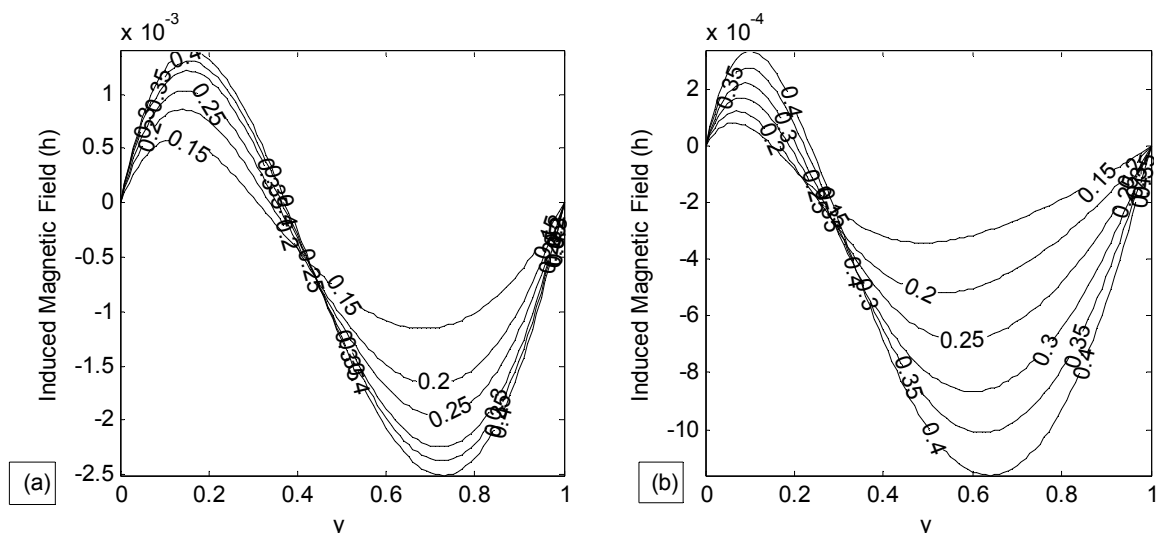
Fig.6. Induced magnetic field profiles at different values of time (*t*) for *M=0.5*, Pr=*0.71* (a) and *7.0* (b).
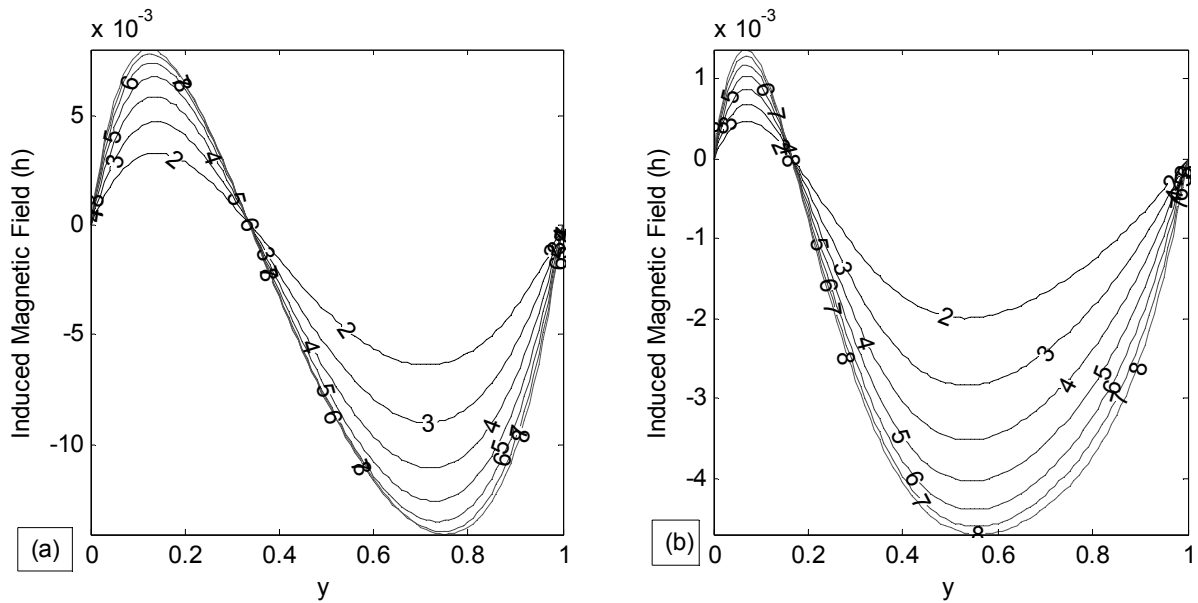
Fig.7. Induced magnetic field profiles at different values of *M* for *t=0.2*, Pr=*0.71* (a) and *7.0* (b).
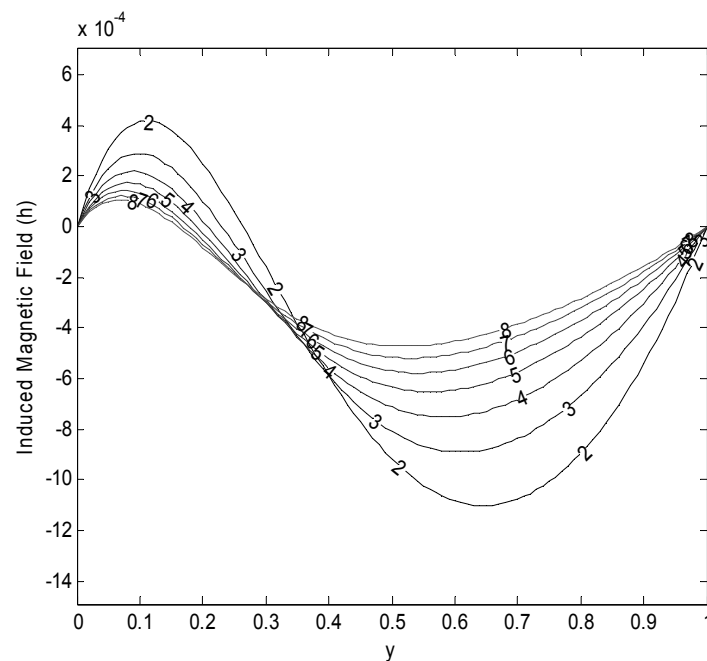
Fig.8. Induced magnetic field profiles at different values of Pr for *t=0.2*, *M=0.5*.

Figures 9-11 depict the current density distribution. From Figs 9a and 9b it is seen that an increase in the dimensionless time (*t*) increases the current density in the range *0.2 < y < 0.8* and *0.15 < y < 0.7* in the case of air and water, respectively, while it decreases with an increase of time near the walls *y=0* and *y=1*. In Figs 10a and 10b a similar trend as in Fig.9 for the effect of the magnetic parameter (*M*) on the current density is observed with a little shift in point of inflection. The current density decreases with an increase in Pr in the central region of the channel while it increases near the channel walls as shown in Fig.11. It is interesting to note that the current density changes its behaviour at two different locations inside the flow domain for all considered values of Pr.

Skin-friction values at both plates *y=0* and *y=1* are plotted against *M* in Figs 12, 13, 15 and 16. Figures 12a and 12b show the skin-friction (τ_0) behavior corresponding to air and water, respectively. It is observed that the skin-friction at *y=0* increases with time, while it decreases as *M* increases. An opposite behavior to this is noticed at the wall *y=1* (Fig.15). Figure 13 shows that the skin-friction at *y=0* decreases with an increase of *M* and Pr for fixed time (*t=0.2*) while a reverse trend is observed in the case of skin-friction at *y=1* (Fig.16). In Fig.14, the skin-friction (τ_0) is plotted against Pr at different values of time (*t*) for the fixed magnetic parameter (*M=0.5*). From this figure, it is observed that the skin-friction (τ_0) increases as time increases while it decreases as Pr increases. A similar behavior is observed in the case of (τ_1) as seen in Fig.17.
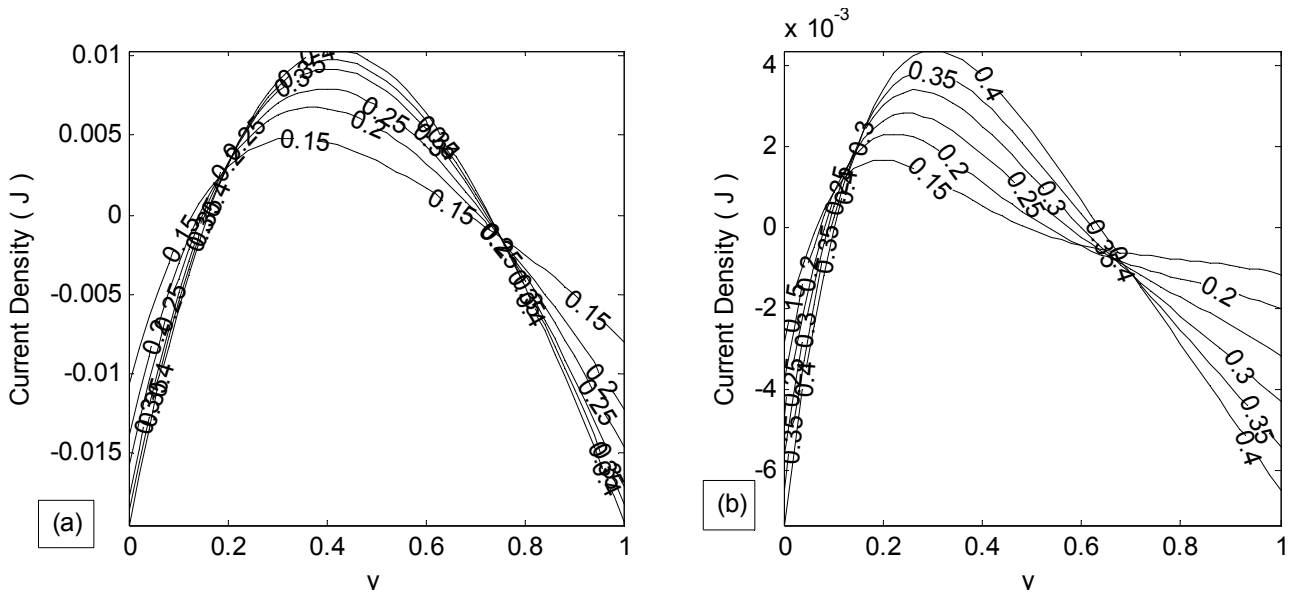
Fig.9. Current density profiles at different values of time *t* for *M=0.5*, Pr=*0.71* (a) and *7.0* (b) respectively.
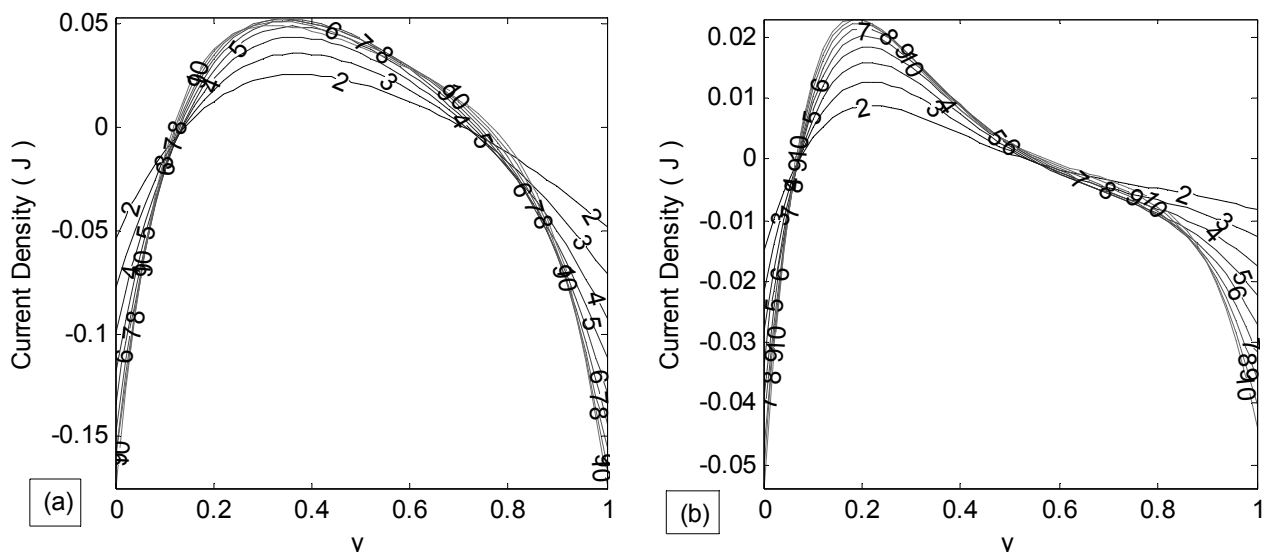
Fig.10. Current density profiles at different values of *M* for *t=0.2*, Pr=*0.71* (a) and *7.0* (b).
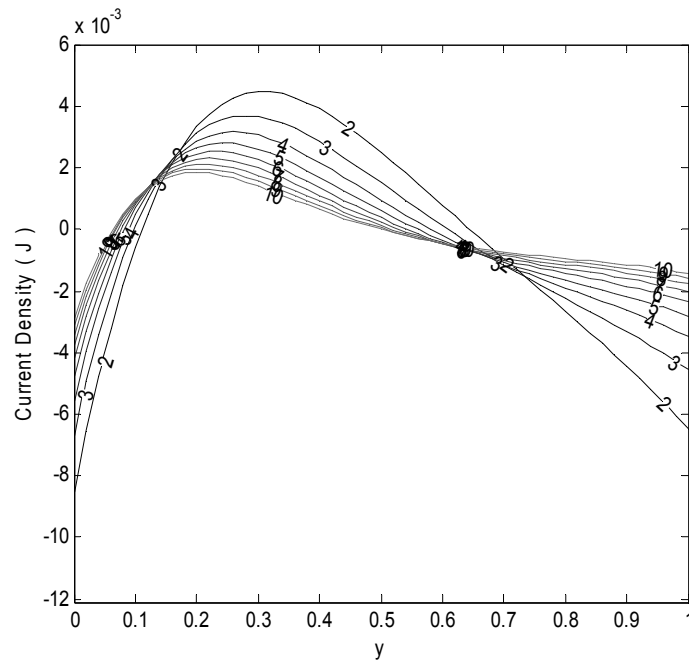
Fig.11. Current density profiles at different values of Pr for *t=0.2, M=0.5*.
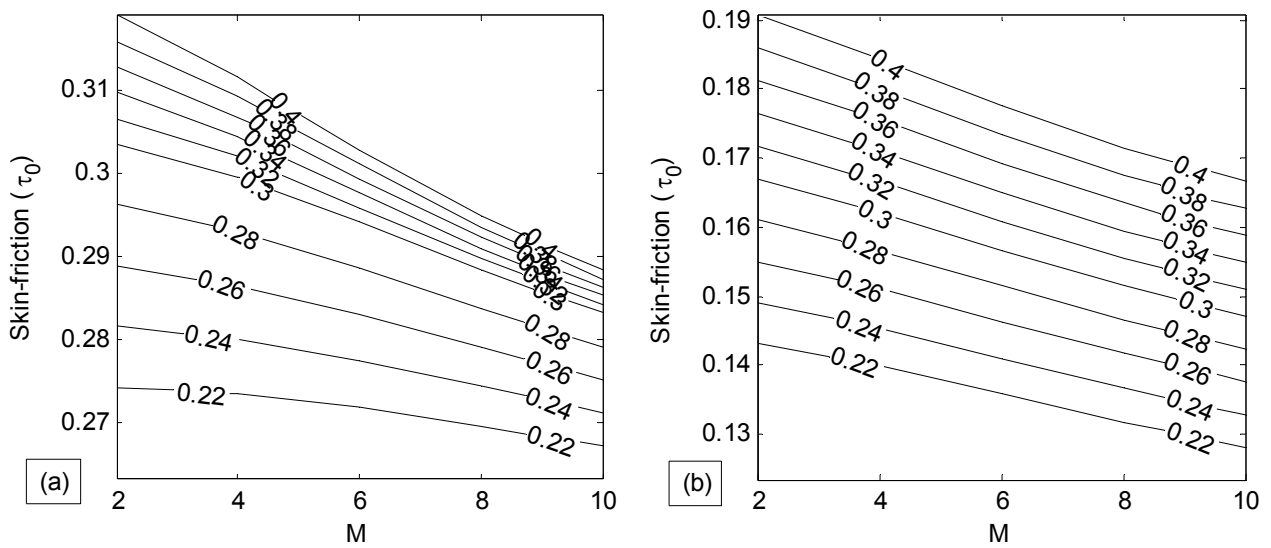
Fig.12. Skin-friction $\left(\tau_0\right)$ against *M* at different values of time $\left(t\right)$ for Pr=*0.71* (a) and *7.0* (b).
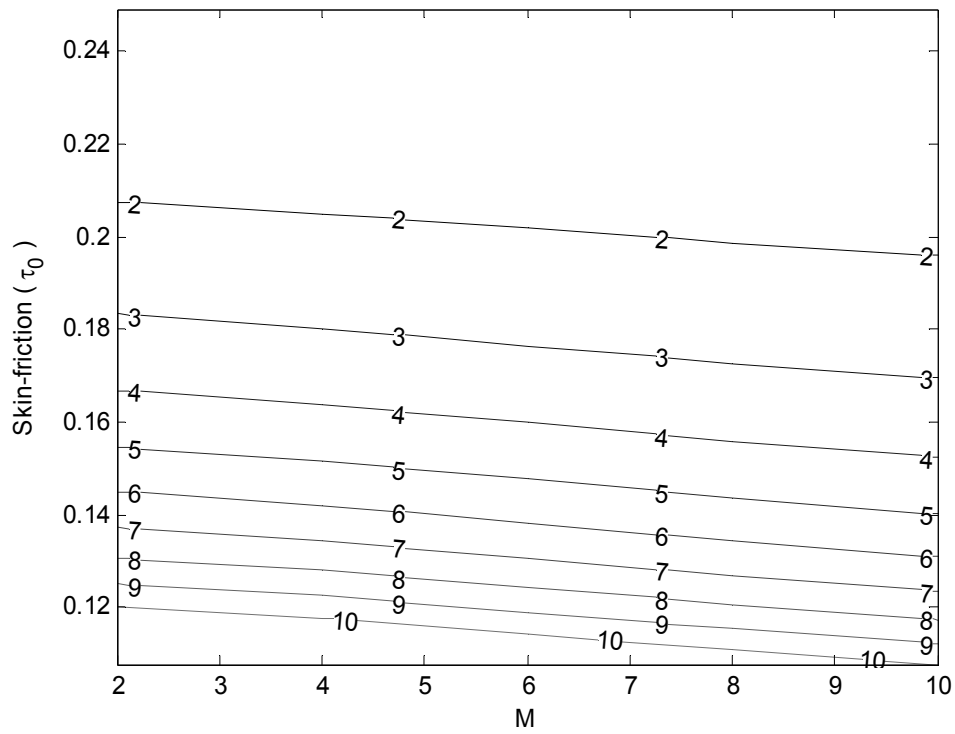
Fig.13. Skin-friction (τ_0) against *M* at different values of Pr for *t=0.2.*
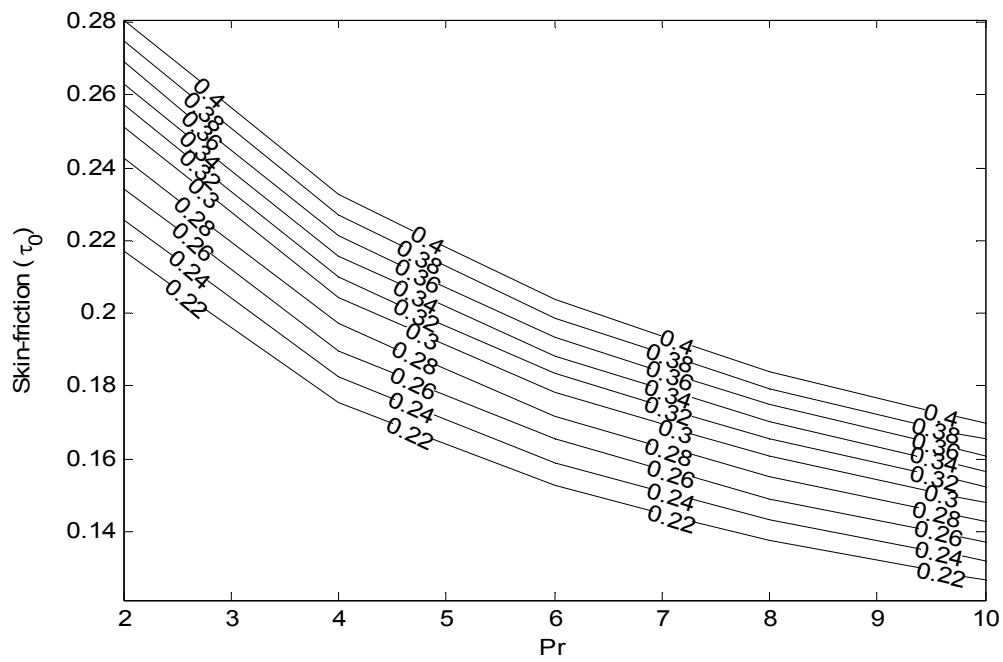
Fig.14. Skin-friction (τ_0) against Pr at different values of *t* for *M=0.5.*
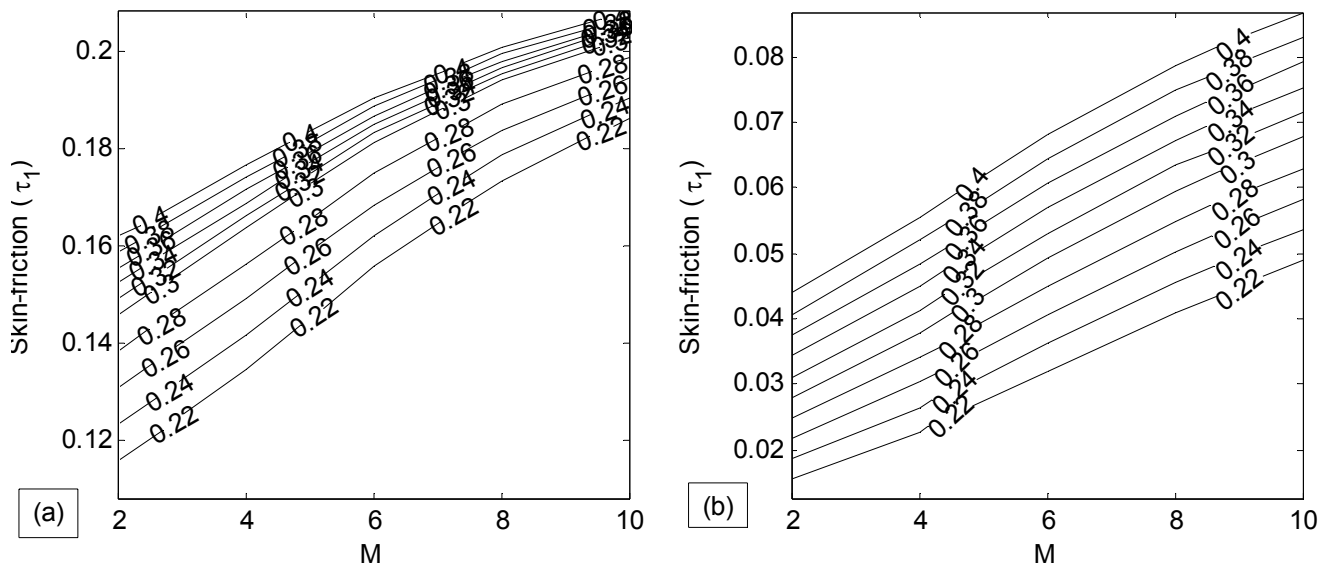
Fig.15. Skin-friction (τ_1) against M at different values of time t for Pr=0.71 (a) and 7.0 (b).

Fig.16. Skin-friction (τ_1) against M at different values of Pr for $t=0.2$.

Fig.17. Skin-friction $\left(\tau_1\right)$ against Pr at different values of *t* for *M=0.5*.

Tables 1 and 2 show a comparison of the transient state and steady state numerical values of velocity and the induced magnetic field obtained by using the Riemann-sum approximation method (RSM), finite difference method (FDM) and exact solution for the steady state (SS) at varying values of time (*t*) for Pr = *0.71*, Pm = *1.0* and *M = 0.5*. This shows an excellent agreement between the three methods at large values of time. Table 3 shows the numerical values of the velocity and the induced magnetic field obtained by the implicit finite difference method at varying values of the magnetic Prandtl number Pm and fixed values of Pr = *0.71*, *M = 0.5*, and *t = 0.2*. It is found that as Pm increases the velocity increases while the induced magnetic field decreases.

Table 1. Numerical values of the flow velocity $\left(u\right)$ obtained using the Riemann-Sum approximation method (RSM) compared to those obtained by the finite difference method (FDM) and the steady state (SS) for Pr=*0.71*, Pm=*1.0* and *M=0.5* at varying values of *t*.

y	*t=0.2*		*t=0.4*		*t=0.6*		SS
	RSM	FDM	RSM	FDM	RSM	FDM	
0.0	*0.0000*	*0.0000*	*0.0000*	*0.0000*	*0.0000*	*0.0000*	*0.0000*
0.1	*0.0219*	*0.0219*	*0.0273*	*0.0273*	*0.0283*	*0.0283*	*0.0284*
0.2	*0.0355*	*0.0355*	*0.0457*	*0.0457*	*0.0475*	*0.0475*	*0.0478*
0.3	*0.0422*	*0.0423*	*0.0563*	*0.0563*	*0.0588*	*0.0588*	*0.0592*
0.4	*0.0437*	*0.0438*	*0.0602*	*0.0602*	*0.0631*	*0.0632*	*0.0637*
0.5	*0.0412*	*0.0413*	*0.0585*	*0.0586*	*0.0616*	*0.0616*	*0.0622*
0.6	*0.0358*	*0.0359*	*0.0523*	*0.0523*	*0.0552*	*0.0552*	*0.0557*
0.7	*0.0283*	*0.0284*	*0.0424*	*0.0424*	*0.0449*	*0.0449*	*0.0453*
0.8	*0.0195*	*0.0196*	*0.0298*	*0.0298*	*0.0316*	*0.0316*	*0.0319*
0.9	*0.0997*	*0.0100*	*0.0154*	*0.0154*	*0.0163*	*0.0163*	*0.0165*
1.0	*0.0000*	*0.0000*	*0.0000*	*0.0000*	*0.0000*	*0.0000*	*0.0000*

Table 2.   Numerical values of the induced magnetic field (h) obtained using the Riemann-Sum approximation method (RSM) compared to those obtained by the finite difference method (FDM) and the steady state (SS) for Pr=*0.71*, Pm=*1.0* and *M=0.5* at varying values of *t*.

	t=0.2		*t=0.4*		*t=0.6*		SS
y	RSM	FDM	RSM	FDM	RSM	FDM	
0.0	*0.0000*	*0.0000*	*0.0000*	*0.0000*	*0.0000*	*0.0000*	*0.0000*
0.1	*0.0008*	*0.0008*	*0.0012*	*0.0012*	*0.0013*	*0.0013*	*0.0013*
0.2	*0.0008*	*0.0008*	*0.0013*	*0.0013*	*0.0015*	*0.0014*	*0.0015*
0.3	*0.0002*	*0.0002*	*0.0007*	*0.0007*	*0.0008*	*0.0008*	*0.0008*
0.4	*-0.0004*	*-0.0004*	*-0.0003*	*-0.0002*	*-0.0002*	*-0.0002*	*-0.0002*
0.5	*-0.0010*	*-0.0010*	*-0.0013*	*-0.0012*	*-0.0012*	*-0.0012*	*-0.0013*
0.6	*-0.0015*	*-0.0015*	*-0.0020*	*-0.0020*	*-0.0022*	*-0.0022*	*-0.0022*
0.7	*-0.0017*	*-0.0017*	*-0.0025*	*-0.0025*	*-0.0026*	*-0.0026*	*-0.0027*
0.8	*-0.0015*	*-0.0015*	*-0.0023*	*-0.0023*	*-0.0025*	*-0.0025*	*-0.0025*
0.9	*-0.0010*	*-0.0010*	*-0.0015*	*-0.0015*	*-0.0017*	*-0.0016*	*-0.0017*
1.0	*0.0000*	*0.0000*	*0.0000*	*-0.0000*	*0.0000*	*0.0000*	*0.0000*

Table 3. Numerical values for velocity (u) and that of the induced magnetic field (h) obtained by the finite difference method for Pr=*0.71*, Pm=*1.0*, *t=0.2* at varying values of *M*.

	M=0.5		*M=1.0*		*M=1.5*	
y	*u*	*h*	*u*	*h*	*u*	*h*
0.0	*0.0000*	*0.0000*	*0.0000*	*0.0000*	*0.0000*	*0.0000*
0.1	*0.0219*	*0.0008*	*0.0218*	*0.0016*	*0.0217*	*0.0023*
0.2	*0.0355*	*0.0008*	*0.0353*	*0.0015*	*0.0350*	*0.0022*
0.3	*0.0422*	*0.0002*	*0.0419*	*0.0005*	*0.0415*	*0.0007*
0.4	*0.0437*	*-0.0004*	*0.0434*	*-0.0008*	*0.0429*	*-0.0012*
0.5	*0.0412*	*-0.0010*	*0.0409*	*-0.0021*	*0.0404*	*-0.0030*
0.6	*0.0358*	*-0.0015*	*0.0356*	*-0.0029*	*0.0353*	*-0.0043*
0.7	*0.0283*	*-0.0017*	*0.0282*	*-0.0033*	*0.0281*	*-0.0049*
0.8	*0.0195*	*-0.0015*	*0.0196*	*-0.0030*	*0.0196*	*-0.0044*
0.9	*0.0997*	*-0.0010*	*0.0100*	*-0.0019*	*0.0102*	*-0.0029*
1.0	*0.0000*	*0.0000*	*0.0000*	*-0.0000*	*0.0000*	*0.0000*

4.   Conclusions

1. Velocity of the fluid increases with an increase in time (*t*) while decreases with an increase in the value of the Prandtl number (Pr).
2. The skin-friction attains a steady state faster in the case of air (Pr = *0.71*) than water (Pr = *7.0*).
3. The impact of the magnetic Prandtl number on the induced magnetic field is pronounced while it is not significant on the velocity field for the considered values of Pm.
4. As *M* increases, velocity decreases near the hot plate *y = 0*, while it increases near the cold plate *y = 1*.
5. As time increases, the current density increases in the central region of the channel while it decreases near both boundaries.

Acknowledgement

Nomenclature

g – acceleration due to gravity
H_0 – applied magnetic field
h – dimensionless induced magnetic field
h' – induced magnetic field
J – current density
M – magnetic parameter
Pm – magnetic Prandtl number
Pr – Prandtl number
T' – temperature of the fluid
t – dimensionless time
t' – dimensional time
u – dimensionless velocity
u' – dimensional velocity
y – dimensionless coordinate normal to the channel plates
y' – dimensional coordinate normal to the channel plates
α – thermal diffusivity of fluid
β – coefficient of thermal expansion
ρ – density
σ – electric conductivity
ν – kinematic viscosity
μ_e – magnetic permeability
θ – dimensionless temperature

References

Anwar B.O., Bakier A.Y., Prasad V.R., Zueco J. and Ghosh S.K. (2009): *Nonsimilar, laminar, steady, electrically-conducting forced convection liquid metal boundary layer flow with induced magnetic field effects.* – International. J. Thermal Sciences, vol.48, No.8, pp.1596-1606.

Attia H.A. (1998): *Hall current effects on the velocity and temperature fields of an unsteady Hartmann flow.* – Canadian Journal of Physics, vol.76, No.9, pp.739-746.

Attia H.A. (2004): *Unsteady Hartmann flow of a viscoelastic fluid considering the Hall effect.* – Canadian Journal of Physics, vol.82, pp.127-136.

Aung W. (1972): *Fully developed laminar free convection between vertical plates heated asymmetrically.* – International J. Heat and Mass Transfer, vol.15, pp.1577-1580.

Ghosh S.K., Beg O.A. and Zueco J. (2010): *Hydromagnetic free convection flow with induced magnetic field effects.* – Mechanica, vol.45, No.2, pp175-185.

Ghosh S.K and Bhattacharjee P.K. (2000): *Hall effects on steady hydromagnetic flow in a rotating channel in the presence of an inclined magnetic field.* – Czech. Journal of Physics, vol.50, pp.759-768.

Gupta A.S., Mishra J.C. and Reza M. (2005): *Magnetohydrodynamic shear flow along a flat plate with uniform suction or blowing.* – Zeitschrift für Angewandte Mathematik fund Physik (ZAMP) vol.56, No.6, pp.1030-1047.

Hartmann J. (1937): *Hg-dynamics-I, theory of laminar flow of an electrically conducting liquid in a homogeneous magnetic field.* – Part I, Journal of Mathematical Physics, Copenhagen, vol.15, No.6.

Jha B.K. and Apere C.A. (2010): *Unsteady MHD Couette flows in an annulli, the Riemann-Sum approximation approach*. – Journal of Physical. Society of Japan, vol.79, pp.124403 /1-5.

Jha B.K. and Apere C.A. (2011): *Magnetohydrodynamics free convective Couette flow with suction and injection*. – Trans. ASME, J. Heat Transfer, vol.133, pp1-12.

Jha B.K. and Apere C.A. (2012): *Magnetohydrodynamic transient free convective flow in a vertical annulus with thermal boundary condition of the second kind*. – Trans. ASME, J. Heat Transfer, vol.134, No.4, pp15/1.4005109.

Jha B.K., Singh A.K. and Takhar H.S. (2003): *Transient free convection flows in vertical channel due to symmetric heating*. – International Journal of Applied Mechanics and Engineering, vol.8, No.3, pp.497-502.

Joshi H.M. (1988): *Transient effects in natural convection cooling of vertical parallel plates*. – International Communications in Heat and Mass Transfer, vol.15, No.2, pp.227-238.

Koshiba Y., Matsushita T. and Ishikawa M. (2002): *Influence of induced magnetic field on large-scale pulsed MHD generator*. – AIAA 33rd Plasma Dynamics and Lasers Conference, Maui, Hawaii.

Krishna G.S. (2009): *Analytical solution to the problem of MHD free convective flow of an electrically conducting fluid between two heated parallel plates in the presence of an induced magnetic field*. – International Journal of Applied Mathematics and Computation, vol.1, No.4, pp.183-193.

Mishra S.P. and Mohapatra P. (1975): *Unsteady free convection flow from a vertical plate in the presence of a uniform magnetic field*. – ZAMM, vol.55, pp.759-762.

Nadeem S. and Akbar N.S. (2010): *Effects of induced magnetic field on peristaltic flow of Johnson-Segalman fluid in a vertical symmetric channel*. – Appl. Math. Mech. -Engl. Ed. vol.31, No.8, pp.969-978.

Oreper G.M. and Szekely J. (1983): *The effect of an externally imposed magnetic field on buoyancy driven flow in rectangular cavity*. – Journal of Crystal Growth, vol.64, pp.505-515.

Ostrach S. (1952): *Laminar natural-convection flow and heat transfer of fluids with or without heat sources in channels with constant wall temperatures*. – NASA, Report No. NACA-TN -2863.

Osterle J.F. and Young F.J. (1961): *Natural convection between heated vertical plates in horizontal magnetic field*. – Journal of Fluid Mechanics, vol.11, pp.512-518.

Paul T., Jha B.K. and Singh A.K. (1996): *Transient free convection flow in vertical channel with constant heat flux on walls*. – Heat Mass Transfer, vol.32, pp.61-63.

Poots G. (1961): *Laminar natural convection flow in magnetohydrodynamics*. – International Journal. of Heat and Mass Transfer, vol.3, pp.1-25.

Raptis A.A., Perdikis C. and Leontitsis A. (2003): *Effects of radiation in an optically thin gray gas flowing past a vertical infinite plate in the presence of a magnetic field*. – Heat and Mass Transfer, vol.39, pp.771-773.

Romig M.F. (1964): *The influence of electric and magnetic fields on heat transfer to electrically conducting fluids*. – Advances in Heat Transfer, vol.1, pp.267-354.

Rum P., Bhandari A. and Sherman K. (2010): *Effect of magnetic field-dependent viscosity on revolving ferrofluid*. – Journal of Magnetism and Magnetic Materials, vol.322, pp.3475-3482.

Singh A.K. and Paul T. (2006): *Transient natural convection between two vertical walls heated/cooled asymmetrically*. – International Journal of Applied. Mechanics and Engineering, vol.11, No.1, pp.143-154.

Singha K.G. (2009): *Analytical solution to the problem of MHD free convective flow of an electrically conducting fluid between two heated parallel plates in the presence of an induced magnetic field*. – Int. J. Appl. Math. and Computation, vol.1, No.4, pp183-193.

Singh R.K., Singh A.K., Sacheti N.C. and Chandran P. (2010): *On hydromagnetic free convection in the presence of induced magnetic field*. – Heat Mass Tran., vol.46, pp.523-529.

Singh R.K. and Singh A.K. (2012): *Effect of induced magnetic field on natural convection in vertical concentric annuli*. – Acta Mech. Sin., vol.28, No.2, pp.315-323.

Soundalgekar V.M. (1965): *Hydromagnetic flow near an accelerated plate in the presence of a magnetic field.* – Applied Scientific Research, vol.12, pp.151-156.

Takhar H.S., Chamkha A.J. and Nath G. (1999): *Unsteady flow and heat transfer on a semi-infinite flat plate with an aligned magnetic field.* – International. J. Engineering Science, vol.37, No.13, pp.1723-1736.

Tzou D.Y. (1997): *Macro to Microscale Heat Transfer. The Lagging Behavior.* – London: Taylor and Francis.

Appendix

$$c_1 = \frac{1}{2} \frac{1}{s\sinh\left(\sqrt{s\mathrm{Pr}}\right)} \left[\frac{e^{\sqrt{s\mathrm{Pr}}}}{d_1} - \frac{e^{-\sqrt{s\mathrm{Pr}}}}{d_2} \right],$$

$$c_2 = \frac{M\sqrt{s\mathrm{Pr}}\, e^{\frac{M}{2}}}{\sinh(\lambda)\, s\sinh\left(\sqrt{s\mathrm{Pr}}\right)\left[(s\mathrm{Pr}-s)^2 - M^2 s\mathrm{Pr} \right]} - \frac{\cosh(\lambda)}{\sinh(\lambda)} c_1,$$

$$c_3 = \frac{1}{2} \frac{1}{s\sinh\left(\sqrt{s\mathrm{Pr}}\right)} \left[\frac{e^{\sqrt{s\mathrm{Pr}}}}{d_2} - \frac{e^{-\sqrt{s\mathrm{Pr}}}}{d_1} \right],$$

$$c_4 = \frac{-M\sqrt{s\mathrm{Pr}}\, e^{-\frac{M}{2}}}{\sinh(\lambda)\, s\sinh\left(\sqrt{s\mathrm{Pr}}\right)\left[(s\mathrm{Pr}-s)^2 - M^2 s\mathrm{Pr} \right]} - \frac{\cosh(\lambda)}{\sinh(\lambda)} c_3,$$

$$c_5 = \frac{\left[d_4 e^{-M} - d_3 \right] M}{e^{-M} - 1}, \qquad c_6 = \frac{\left[d_3 - d_4 \right]}{e^{-M} - 1}, \qquad c_7 = \frac{\left[d_5 e^{M} - d_6 \right] M}{e^{M} - 1},$$

$$c_8 = \frac{\left[d_5 - d_6 \right]}{e^{M} - 1}, \qquad \lambda = \sqrt{\frac{M}{4} + s}, \qquad d_1 = s\mathrm{Pr} - sM\sqrt{s\,\mathrm{Pr}}, \qquad d_2 = s\mathrm{Pr} + sM\sqrt{s\,\mathrm{Pr}},$$

$$d_3 = \frac{c_5}{M} + c_6 e^{-M}, \qquad d_4 = \frac{c_5}{M} + c_6, \qquad d_5 = \frac{c_7}{M} + c_8, \qquad d_6 = \frac{c_7}{M} + c_8 e^{-M}.$$